Colloids and Surfaces B: Biointerfaces 122 (2014) 19–29

Contents lists available at ScienceDirect

Colloids and Surfaces B: Biointerfaces

journal homepage: www.elsevier.com/locate/colsurfb

Enhanced antimelanoma activity of methotrexate and zoledronic acid within polymeric *sandwiches*

Priscila Schilrreff, Gabriela Cervini, Eder Lilia Romero, Maria Jose Morilla*

Nanomedicine Research Program, Departamento de Ciencia y Tecnologia, Universidad Nacional de Quilmes, Roque Saenz Peña 352, Bernal B1876 BXD, Argentina

ARTICLE INFO

Article history:
Received 29 January 2014
Received in revised form 8 May 2014
Accepted 13 June 2014
Available online 20 June 2014

Keywords:
Melanoma
Dendrimers
Antifolates
Bisphosphonates

ABSTRACT

New therapies are urgently needed against melanoma, one of the most aggressive tumors. Melanoma cells are resistant to the antifolate methotrexate (MTX), since MTX is taken up by the folate receptor-α (FRα), sequestered in melanosomes and exported out of the cell. The bisphosphonate zoledronic acid (ZOL) is active in several non-skeletal tumors; however, its antitumoral activity is hampered by its long-term accumulation in bones and low cellular permeability. Recently, we showed that core–shell tecto-dendrimers made of amine-terminated polyamidoamine generation 5 dendrimer (G5) as core and carboxyl-terminated G2.5 dendrimer as shell (G5G2.5) had selective cytotoxicity to melanoma cells. We hypothesized here that the activity of MTX and ZOL on melanoma cells could be enhanced when loaded within G5G2.5.

MTX and ZOL were loaded within G5 cores, which were coated by a covalently bound shell of G2.5 dendrimers (drug-*sandwiches*). 12 nm mean diameter and −12 mV Z potential drug-*sandwiches* incorporating 6 and 31 molecules of MTX and ZOL, respectively, per G5G2.5, showed higher cytotoxicity (by MTT and apoptosis/necrosis assays) to melanoma (Sk-Mel-28) cells than free drugs and G5G2.5. Only MTX-*sandwich* was cytotoxic to Sk-Mel-28 cells and harmless to keratinocytes (HaCaT cells). The intracellular pathway of G5G2.5 was followed using chemical inhibitors of endocytosis. The increased cytotoxicity of MTX-*sandwich* could be due to its uptake by macropinocytosis instead of by FRα, avoiding MTX exocytosis. The increased cytotoxicity of ZOL-*sandwich* could be due to an increased intracellular accumulation of ZOL, owed by its endocytic uptake instead of diffusing as free drug.

1. Introduction

Malignant melanoma is a tumor of the melanocytes, specialized pigment cells located amongst the basal layer of the epidermis, hair bulb, eyes, ears, and meninges [1–4]. Once detected, primary melanomas are surgically removed and chemotherapy focuses on metastasis control. There are four drugs approved by the Food and Drug Administration for melanoma (dacarbazine, interleukin-2, ipilimumab and vemurafenib). Since 1975 dacarbazine remains the gold standard in chemotherapy, in spite of its response rate of about 10% and a median survival of 8–9 months. High doses of interleukin-2 on the other hand, induce complete and durable responses only in one of twenty patients, while ipilimumab and vemurafenib have raised many hopes in the last few years [5]. However, melanoma remains as one of the most aggressive malignancies in human and is responsible for almost 60% of lethal skin cancer [6]. This scenario clearly highlights the need for alternative therapies against this type of tumor [7].

One complication of melanoma chemotherapy is the limited effectiveness of antifolates. Although methotrexate (MTX), the most frequently used antifolate, is an effective drug against several types of cancer [8,9], it is not active against melanoma [10]. MTX blocks the folate-dependent enzyme dihydrofolate reductase (DHFR), which is a pivotal enzyme in providing purines and pyrimidine precursors for the biosynthesis of DNA, RNA and amino acids. The mechanism of MTX resistance in melanoma cells involves its sequestration in specialized organelles known as melanosomes where melanin synthesis occurs, and the subsequent exportation of MTX-containing melanosomes out of the cell [11]. This mechanism, also described for cisplatin [12,13], is mediated by the uptake of MTX by a glycosylphosphatidylinositol (GPI)-anchored protein, the folate receptor-α (FRα). The subsequent expulsion of

* Corresponding author. Tel.: +54 1143657100; fax: +54 1143657132.
E-mail address: jmorilla@unq.edu.ar (M.J. Morilla).

http://dx.doi.org/10.1016/j.colsurfb.2014.06.033
0927-7765/

MTX reduces its accumulation in the cytosol of melanoma cells and impedes the FRα recycling to the cell membrane, making melanoma cells impermeable to folates. We hypothesize that a MTX delivery system, capable of modifying its uptake pathway within melanoma cells by avoiding its expulsion, could enhance its toxicity.

On the other hand, the nitrogenous-containing bisphosphonate zoledronic acid (ZOL) is a potent inhibitor of the farnesyl pyrophosphate synthase, interfering with the mevalonate pathway and related critical processes in cell signaling and growth [14,15]. ZOL has high affinity for the bone mineral matrix and is a potent inhibitor of osteoclast proliferation. Additionally, ZOL has anti-angiogenic and anti-tumoral effect in several non-skeletal tumor models, including breast cancer and myeloma. Currently, ZOL is in clinical use against osteoporosis, breast cancer patients with bone metastases and Paget's disease [16–19]. Nonetheless, the antitumor efficacy of ZOL on tumors other than those from skeletal origin is limited by its fast blood clearance, long-term accumulation in bone tissues and low cellular permeability. In contrast to MTX, ZOL does not employ specific transporters to enter the cells. Therefore, a ZOL delivery system that overcomes its low permeability could enhance its toxicity in melanoma cells.

We have recently shown that *in vitro*, core–shell tecto-dendrimers made of amine-terminated polyamidoamine (PAMAM) generation 5 (G5) as core and carboxyl-terminated PAMAM generation 2.5 (G2.5) as shell (G5G2.5), are cytotoxic to melanoma cells and not to keratinocytes [20]. On these bases, in this work we investigated if the low activity against melanoma cell of MTX and ZOL could be enhanced when loaded within G5G2.5. To that aim, we prepared and characterized non-covalent drug-tecto-dendrimer complexes (*sandwiches*) by incorporating MTX and ZOL within G5 cores, which were further coated with a covalently bound shell of G2.5 dendrimers. The cytotoxicity of these *sandwiches* on melanoma cells (Sk-Mel-28) and keratinocytes (HaCaT cells) was tested by MTT and apoptosis/necrosis assays. Additionally, a set of chemical inhibitors of endocytosis was used to assess the uptake mechanism of G5G2.5 by melanoma cells.

2. Material and methods

2.1. Materials

Ethylendiamine core PAMAM G5, G2.5 and G6.5 dendrimers were purchased from Sigma-Aldrich (St Louis, MO). Methotrexate, LiCl, 1-(3-dimethylaminopropyl)-3-ethylcarbodiimide hydrochloride (EDC), fluorescein isothiocyanate isomer I (FITC), 3-(4,5-dimethylthiazole-2-yl)-2,5-diphenyltetrazolium bromide) (MTT), propidium iodide, Sephadex G25, chloroquine diphosphate salt, cytochalasin D from *Zygosporium mansonii*, genistein and wortmannin from *Penicillium funiculosum* were purchased from Sigma-Aldrich. Nocodazole and methyl-β-cyclodextrin were acquired from Fluka (Buenos Aires, Argentina). Chlorpromazine and zoledronic acid were a gift from Laboratorios Ceballos and Laboratorios Gador SA, Argentina, respectively.

LysoTracker Red DND-99, BODIPY® FL C5-lactosylceramide complexed to bovin serum albumin (LacCer), Alexa Fluor 568 conjugated dextran of 10.000 molecular weight (Dex-Alexa 568) and Alexa Fluor 555 conjugated human serum transferrin (Tf-Alexa-555) were from Molecular Probes (Eugene, OR). Modified Eagle's medium (MEM) and L-glutamine were from Gibco, Life Technologies (Eugene, OR). Fetal bovine serum (FBS), trypsin-EDTA solution and antibiotic/antimycotic solution were obtained from PAA Laboratories (Pasching, Austria). The other reagents were analytic grade from Anedra, Research AG (Buenos Aires, Argentina).

2.2. Preparation and characterization of MTX- and ZOL-sandwiches

2.2.1. Preparation

G5G2.5 was synthesized and purified as described in Shilrreff et al. [20]. To obtain MTX- and ZOL-*sandwiches*, drugs were incubated with G5 before the covalent linkage of G5G2.5. First, increasing amount of drugs (1 and 2 mg of MTX and 2, 4 and 8 mg of ZOL) dissolved in two different media (MilliQ water or 23 mg/ml LiCl aqueous solution) was incubated with 1 mg (0.04 μmol) G5 for 15 h under stirring at 250 rpm. The samples were centrifuged at 10,000 rpm, and MTX and ZOL in supernatant were quantified as described in the following section. *Sandwiches* were prepared employing the medium rendering highest drug payload. Hence, 2 mg MTX (4.4 μmol) or 4 mg ZOL (13.8 μmol) were incubated with 1 mg of G5 (0.04 μmol) in 23 mg/ml LiCl for 15 h under stirring at 250 rpm. Thereafter, 7.5 mg (1.2 μmol) of G2.5 in MilliQ water was added at a 1:30. G5:G2.5 molar ratio. The mixture was allowed to equilibrate for 20 h at room temperature. Subsequently, the linking reagent EDC (11.5 mg) was added and the reaction mixture was incubated by 6 h. Finally, each mixture was dialyzed using a 12,000-Da cutoff cellulose membrane against 80 volumes of 10 mM Tris–HCl pH 7.4 buffer (Tris–HCl buffer) for 5 h and fractionated on Sephadex G25 chromatographic column to separate free drugs from that in G5-drug-G2.5 *sandwiches*. Samples were collected, lyophilized (−50 °C, 10^{-3} mbar) and stored at 4 °C.

2.2.2. MTX and ZOL quantification

MTX was quantified by measuring its absorbance at 304 nm. The calibration curve of MTX in 250 mM carbonate buffer pH 9.1 was linear in a concentration range of 25–8 μg/ml (r^2 = 0.9907). ZOL contains two phosphorus atoms per molecule, and was quantified by measuring phosphate content by Bötcher assay [21]. The calibration curve of ZOL in Tris–HCl buffer was linear in a concentration range of 20–2 μg/ml (r^2 = 0.9971).

2.2.3. G5G2.5 quantification

The yield of each batch was determined by densitometry using G6.5 as standard. Increasing amounts of G6.5 (1–8 μg), G5G2.5 and drug-*sandwiches* were run in 15% PAGE using TBE buffer pH 8.3 (0.089 M Tris, 0.089 boric acid, 2 mM EDTA). Gels were run at a constant voltage of 200 V. Gels were stained with 0.1% Coomassie brilliant blue R-250 in 20% (v/v) methanol and 10% (v/v) acetic acid and destained in the same solution (without the dye) to visualize polymers bands. Images were obtained and band intensity was determined by ImageJ software (National Institute of Health, Bethesda, MD). A plot of G6.5 mass (in micrograms) *versus* band intensity was fitted by linear regression.

2.2.4. Size and Z potential

Size and zeta potential of drug-*sandwiches* in Hank's balanced salt solution (HBSS) were determined by dynamic light scattering and phase analysis light scattering, respectively, using a Nanosizer (ZEN 3600; Malvern Instruments, Malvern, UK).

2.2.5. FTIR spectroscopy

FTIR spectra of MTX, ZOL, G5G2.5, G5, G2.5, MTX- and ZOL-*sanwiches* were measured using a FTIR Nicolet 8700 spectrometer equipped with a single reflection diamond Attenuated Total Reflectance (ATR) accessory. Samples were prepared by dispersion of lyophilized solids in potassium bromide followed by vacuum press. Spectra were run between 525 and 4000 cm^{-1} with a resolution of 4 cm^{-1}, at 64 scans per sample. Spectra were analyzed with OMNIC version 7.3 Thermo Electron Corporation.

2.3. Cytotoxicity of MTX- and ZOL-sandwiches

2.3.1. Cells

Human melanoma cells Sk-Mel-28 (ATCC, HTB-72™), were obtained from the Asociación Banco Argentino de Células. Dr. Edgardo Salvatierra, Instituto Leloir, Argentina, kindly provided immortalized human nontumorigenic keratinocites HaCaT. Cells were routinely culture in MEM supplemented with 10% (v/v) FBS, 1% (v/v) antibiotic/antimycotic solution and 2 mM glutamine, at 37 °C in 5% CO_2 and 95% humidity.

2.3.2. MTT assay

Cell viability upon treatment with G5G2.5, MTX, ZOL, MTX- and ZOL-*sandwiches* was measured by MTT assay. Cells were seeded at a density of 3×10^4 cells/well in 96-well plates and allowed to attach overnight. The medium was then replaced with fresh medium with 5% FBS containing increasing concentrations of: G5G2.5 from 2 to 16 μM; MTX from 12 to 100 μM; ZOL from 62 to 500 μM; MTX-*sandwich* from 12 to 100 μM MTX and 2 to 16 μM G5G2.5; and ZOL-*sandwich* from 62 to 500 μM ZOL and 2 to 16 μM G5G2.5. Upon incubating 24 h at 37 °C, the medium was removed and replaced by 0.5 mg/ml of MTT. Four hours later, MTT solution was removed, the insoluble formazan crystals were dissolved in DMSO and absorbance was measured at 570 nm in a microplate reader (Dynex Technologies, modelo MRX tc). The cells viability was expressed as a percentage of the cells grown in medium viability. Assays were carried out in triplicate. Additionally, cellular morphology was examined with an inverted microscope Leica DMI6000 B.

2.3.3. Apoptosis/Necrosis assay

A double staining with YO-PRO-1® and propidium iodide (PI) was used to distinguish between apoptotic and necrotic Sk-Mel-28 cells upon treatment with G5G2.5, MTX, ZOL, MTX- and ZOL-*sandwiches*. This assay detects changes in cell membrane permeability with YO-PRO-1® dye, a green-fluorescent nucleic acid stain that is permeant to apoptotic cells but not to live cells. Necrotic cells were stained with red fluorescent PI.

Cells were seeded at a density of 3×10^5 cells/well in 6-well plates and allowed to grow for 24 h. The medium was then replaced with fresh medium with 10% FBS containing 50 μM MTX, 8 μM G5G2.5, 50–8 μM MTX-*sandwiches* (50 μM MTX and 8 μM G5G2.5), 250 μM ZOL or 250–8 μM ZOL-*sandwiches* (250 μM ZOL and 8 μM G5G2.5), and cells were incubated at 37 °C in a 5% CO_2 humidified incubator. After 7 and 15 h of exposure to MTX and MTX-*sandwiches*, or 24 and 48 h of exposure to ZOL and ZOL-*sandwiches*, the media were removed, cells washed with PBS and collected into Eppendorf tubes by trypsin treatment. Then trypsin was inactivated, the cells washed twice with PBS by centrifugation ($1000 \times g$ for 5 min at 4 °C), and cell density adjusted to 1×10^6 cells/mL in PBS. The cells were incubated with 1 μl of YO-PRO-1® 100 μM for 15 min and 1 μl of PI 0.01 mg/mL for 2 min. The stained cells were analyzed within 1 h by flow cytometry (FACSCAlibur), using 488 nm excitation with green fluorescence emission for YO-PRO-1® (530 nm FL1) and red fluorescence emission for PI (575 nm, FL3). A total of 1×10^4 cells were analyzed, and data processed using WinMDI 2.9 software. Assay was carried out in triplicate.

2.4. Uptake and intracellular traffic of G5G.25

2.4.1. Cytotoxicity of inhibitors of endocytosis

Cell viability upon treatment with inhibitors of endocytosis and G5G2.5 or G6.5 was measured by MTT assay. Cells were seeded at a density of 3×10^4 cells/well in 96-well plates and allowed to attach overnight. The medium was then replaced with HBSS containing the following inhibitors: (i) chlorpromazine (Cpz) 5, 10, 30 μM; (ii) genistein (Gen) 20, 50, 100 μM for Sk-Mel-28 cells and 150, 200, 300 μM for HaCaT cells; (iii) methyl-β-cyclodextrin (MβCD) 0.5, 5, 10 mM for Sk-Mel-28 cells and 7.5, 10 mM for HaCaT cells; (iv) chloroquine (CQ) 5, 10, 50 μM for Sk-Mel-28 and 75, 150 μM for HaCaT cells; (v) nocodazole (Noc) 5, 10, 50 μM for Sk-Mel-28 and 10, 30, 50 μM for HaCaT cells; (vi) cytochalasin D (CytD) 5, 10, 25 μM; (vii) wortmannin (Wort) 50, 200, 500 nM. After 30 min of incubation at 37 °C, G5G2.5 or G6.5 at 7.5 μM were added, followed by 2 h incubation. After that, the medium was removed and cells were processed for MTT assay as described in Section 2.3.2.

2.4.2. Uptake of G5G2.5-FITC and G6.5-FITC in presence of inhibitors of endocytosis

G5G2.5 and G6.5 were labeled with FITC (G5G2.5-FITC or G6.5-FITC), purified and characterized, as described by Schilrreff et al. [20]. HaCaT and Sk-Mel-28 cells were seeded at a density of 1×10^5 cells/well in 24-well plates and allowed to attach overnight. The medium was then replaced with fresh HBSS containing endocytic inhibitors at nontoxic concentrations. The cells were incubated 30 min at 37 °C, then 7.5 μM G5G2.5-FITC or G6.5-FITC was added and the cells were incubated for another 2 h. After incubation, the medium was removed, the cells were washed with phosphate-buffered saline pH 7.4 (PBS), and harvested by trypsinization. After washing with PBS, a total of 1×10^4 cells were analyzed by flow cytometry (Becton Dickinson FACSCalibur, San Jose, CA). Data were analyzed using WinMDI 2.9 software. To read the fluorescence of internalized polymers only, the cells were previously treated with trypan blue in order to quench the external fluorescence.

The percentage of cellular internalization was calculated on the basis of the geometric mean (Gm), as follows: (Gmobs/Gmcontrol) × 100; where Gmobs is the Gm of cells incubated with inhibitors and G5G2.5-FITC or G6.5-FITC and Gmcontrol is the Gm of cells incubated with G5G2.5-FITC or G6.5-FITC.

The activity of the inhibitors chlorpromazine and wortmannin was checked by measuring the uptake of Tf-Alexa-555 (40 μg/ml) and Dex-Alexa-568 (500 μg/ml), as markers of clathrin-dependent endocytosis and macropinocytosis, respectively. The activity of the inhibitors nocodazole and chloroquine could not be checked since commercial markers of microtubules and lysosomal disruption respectively are not available.

2.4.3. Co-localization of G5G2.5-FITC with dextran and lysotracker

Co-localization of G5G2.5-FITC with Dex-Alexa-568 and LysoTracker Red was followed by confocal laser scanning microscopy. Sk-Mel-28 cells were seeded at a density of 1×10^5 cells/well in 24-well plates with rounded cover slips on the bottom and allowed to attach overnight. Then, the medium was replaced with HBSS containing 7.5 μM G5G2.5-FITC and 500 μg/ml Dex-Alexa-568. After 1 h of incubation at 37 °C, the medium was removed; cells were washed twice with PBS and fixed with 4% formaldehyde in PBS for 25 min at 4 °C. The cells were then washed, the cover slips were mounted on slides with 5 μl of mounting medium, and samples were observed with a Nikon confocal laser microscope.

On the other hand, cells were incubated with 7.5 μM G5G2.5-FITC for 1 h at 37 °C. Thereafter suspensions were removed; cells were washed with PBS, fresh medium with 5% FBS was added and cells were incubated for 3, 5 and 12 h. For endosomal-lysosomal staining, 60 min before incubations were finished 5 μl of 38 μM LysoTracker Red were added. Then cells were processed as stated before.

Pearson's correlation coefficient, which describes the correlation of intensity distribution between channels, and is independent of the intensity of signals, was calculated using Mac Biophotonics MBFImage J software (http://www.macbiophotonics.ca/imagej). Pearson's correlation coefficient values between 0.5 and 1

Table 1
Properties of G5G2.5, MTX- and ZOL-*sandwiches*. Values are expressed as mean ± S.D of three independent measurements.

	Size (nm)	Polydispersity (Pdi)	Z-potential (mV)	Drug concentration in *sandwiches* (μg/ml)	Drug/G5G2.5 molar ratio
G5G2.5	10.56 ± 1.98	0.70	−4.0 ± 0.76	–	–
G5G2.5-MTX	12.00 ± 4.29	0.53	−15.08 ± 5.12	140 ± 21	6.3 ± 2.3
G5G2.5-ZOL	12.51 ± 2.77	0.62	−12.26 ± 3.12	500 ± 35	31.3 ± 9.3
G6.5-MTX	11.5 ± 0.7	0.56	−9.0 ± 1.2	20 ± 18	1 ± 1
G6.5-ZOL	10.8 ± 1.5	0.54	−9.8 ± 1.8	15 ± 12	1 ± 1

indicate colocalization, while values between 0 and 0.5 indicate no colocalization [22].

2.5. Statistical analysis

Statistical analyses were performed by one-way analysis of variance, followed by Dunnett's test using Prisma software (v 4.00; Graphpad Software Corporation, San Diego, CA). Significance levels are shown in the figure legends.

3. Results

3.1. Characterization of MTX- and ZOL-sandwiches

Two strategies were used to load MTX and ZOL within tecto-dendrimers. By the direct one, the co-incubation of drugs dissolved in LiCl or pure water with G5G2.5 did not lead to drug association. By the indirect one, different amounts of drugs were co-incubated with the core dendrimer G5, which was then coated by a covalently linked G2.5 shell. We found that the *sandwiches* structures trapped a higher proportion of drugs dissolved in LiCl than in pure water. The amount of drugs loaded into *sandwiches* increased with the incubation ratio up to 2 mg MTX and 4 mg ZOL per 1 mg of G5. These ratios where used for further *sandwiches* preparation.

When the drugs were incubated with the commercial dendrimer G6.5 (of size and Z potential similar to G5G2.5), nearly one drug molecule remained associated per dendrimer molecule. The high surface group congestion of the G6.5 probably hindered the drug entry to the inner pockets. Because of this the anti-melanoma activity of drugs-G6.5 complexes was not determined.

PAGE analysis of MTX- and ZOL-*sandwiches* showed them running as a diffuse band of relative mobility comparable to that of G5G2.5. Their hydrodynamic radii were also similar to that of G5G2.5, but with a negative Z potential slightly lower than that of G5G2.5. Remarkably, the drug/G5G2.5 molar ratio of ZOL-*sandwich* was five folds higher than that of MTX-*sandwich* (Table 1). A possible reason could the difference in size and shape of both drugs. The molecular weight of ZOL is 290.1 and is a planar molecule; meanwhile the molecular weight of MTX is 454.5 and is an angular molecule. Hence MTX could have more restriction to enter to the G5 pockets. On the other hand, the release kinetics of MTX-*sandwich* showed a burst relase, beeing around of 60% of MTX released in the first 30 min (Fig. 1). Besides, the ZOL-*sandwich* showed a sustained relase, beeing only 25% of ZOL release in the first 30 min.

The FTIR spectra of G5G2.5 (Fig. 2) showed the peaks characteristic of G5 and G2.5 dendrimers (the N—H stretching vibration at 3255 cm^{-1}; the —CH_2— asymmetric and symmetric stretching vibration at 2948 cm^{-1}; the amide I mode at 1636 cm^{-1}; the amide II mode at 1541 and the —CH_2— scissoring vibrations at 1458 cm^{-1}). The most remarkable feature was the presence of the asymmetric stretching peak of the —COO^- at 1375 cm^{-1}, that was absent in the cationic G5. The FTIR spectra of MTX and ZOL showed the peaks characteristics of the two drugs. Remarkably, the FTIR spectra of the *sandwiches* presented the same peaks than G5G2.5, but not those of the free drugs. This could be due to superposition of MTX (1539 cm^{-1}) and ZOL peaks (1050 cm^{-1}, 950 cm^{-1}) observed in the spectra of G5-MTX and G5-ZOL complexes (data not shown), with the amide II peak at 1556 cm^{-1} and the broad peak at 1050 cm^{-1} of G5G2.5. The peaks of the amide II and of the symmetric stretching of —COO^- of the *sandwiches* were shifted to higher wavenumbers (1556–1552 cm^{-1} and 1382 cm^{-1}, respectively), suggesting the presence of ionic interaction between drugs and tecto-dendrimer molecules.

3.2. Cytotoxicity

The viability of HaCaT and Sk-Mel-28 cells after 24 h incubation with free drugs, G5G2.5, MTX- and ZOL-*sandwiches* was determined by measuring the activity of the mitochondrial enzyme succinate dehydrogenase by employing a tetrazolium salt (MTT).

As previously reported between 2 and 12 μM G5G2.5 the viability of HaCaT cells was not significantly reduced, but the viability of Sk-Mel-28 cells was decreased in a concentration dependent fashion [20] (Fig. 3A and B). Sk-Mel-28 cells experienced also important morphological changes such as reduction of cellular volume and loss of the tapering shape of the cells (Fig. 3D).

On the other hand, neither MTX nor its sandwich reduced the viability of HaCaT cells. Nonetheless, at 50 μM the MTX-*sandwich* reduced 80% the viability of Sk-Mel-28 cells, accompanied by the already described morphological changes (Fig. 3F). In contrast, 100 μM MTX did not significantly decrease (15%) the viability of Sk-Mel-28 cells and not cause morphological changes (Fig. 3E).

ZOL did not reduce the cell viability neither of HaCaT nor of Sk-Mel-28 cells at any tested concentrations. Nonetheless, at 500 μM the ZOL-*sandwich* decreased 50% and 85% the viability of HaCat and Sk-Mel-28 cells respectively, accompanied by the already described morphological changes (Fig. 3G and H).

At 8 μM concentration G5G2.5, 250–8 μM ZOL-*sandwich* slightly decreased (25%) the viability of both HaCat and Sk-Mel-28 cells. The 50–8 μM MTX-*sandwich* however, showed a pronounced deleterious effect only on Sk-Mel-28 cells. Its cytotoxicity was not only selective to the malignant cells but owed to the trapped MTX, which in the free form was innocuous to Sk-Mel-28 cells. The 50–8 μM MTX-*sandwich* cytotoxicity was not only three folds higher than the G5G2.5 cytotoxicity, but also enabled MTX to exert its cytotoxicity.

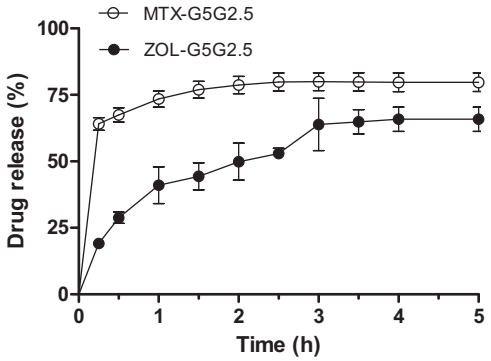

Fig. 1. Drug release kinetic from MTX-and ZOL-*sandwiches*.

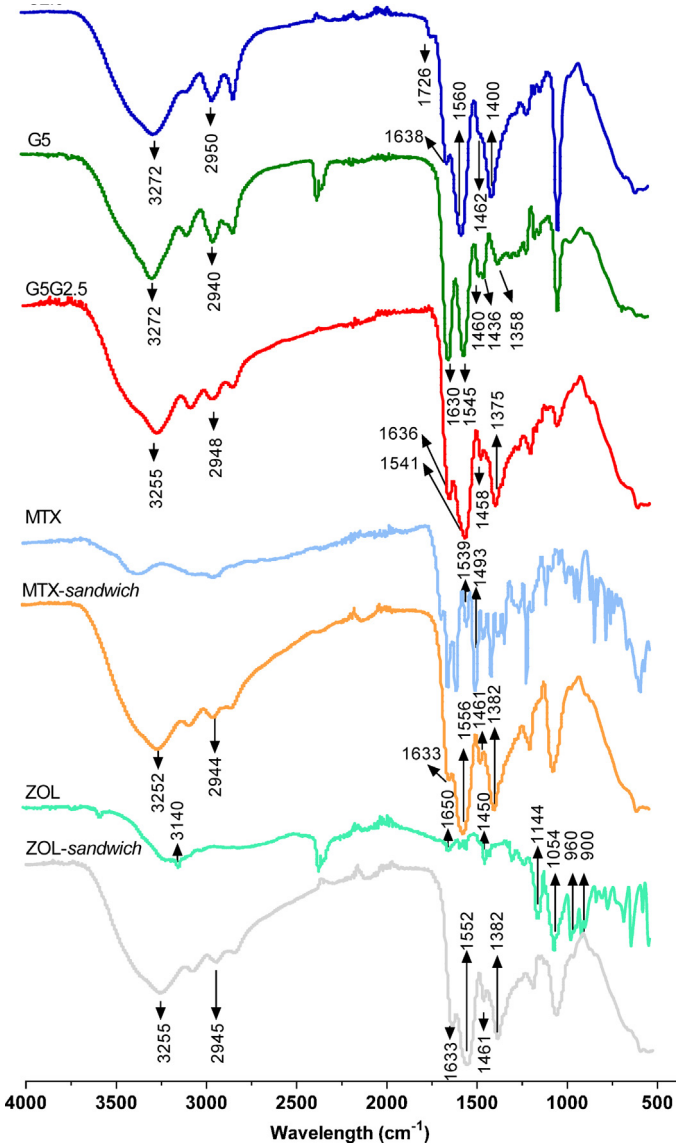

Fig. 2. FTIR spectra of dendrimers, tecto-dendrimers, MTX- and ZOL-*sandwiches*.

Simple mixtures of tecto-dendrimers and drugs showed the same cytotoxicity as tecto-dendrimers alone but lower than that of drug-*sandwiches* on SK-Mel-28 cells (Fig. 3C). These results showed that activity of the drug-loaded tecto-dendrimers is due to greater uptake of each drug-sandwich and not due to any additive effect from both tecto-dendrimers and drugs.

In this context, the relative contribution of apoptosis and necrosis, caused by the 50–8 μM MTX- and 250–8 μM ZOL-*sandwiches* on Sk-Mel-28 cells, was measured by double staining with YOPRO and PI. Since the 50–8 μM MTX-*sandwich* reduced 80% the viability of Sk-Mel-28 cells after 24 h incubation, the assay was carried out at shorter incubation times (7 and 15 h) to detect intermediate stages of cell death process. On the other hand, since the 250–8 μM ZOL-*sandwich* was not cytotoxic, the incubation time was extended for 48 h.

As shown in Fig. 4, 8 μM G5G2.5 reduced 50% cell viability by necrosis, a condition that remained stable in time, with low contribution of apoptosis. However, although MTX did not induce significant cell death, at 50–8 μM MTX-*sandwich* eliminated most viable cells (∼ 6% viable cells) and the remaining cells were in late apoptosis or necrosis after 15 h. This was a significantly higher damage than the produced by G5G2.5. Finally, ZOL did not induce significant cell death and the 250–8 μM ZOL-*sandwich* induced the same damage than G5G2.5. These results were in accordance with the MTT assay and suggested that the death mechanism mainly owed to necrosis.

3.3. Uptake of G5G2.5-FITC in presence of inhibitors of endocytosis and co-localization with biomarkers

The internalization mechanism of G5G2.5-FITC by Sk-Mel-28 and HaCaT cells was screened employing a set of inhibitors of endocytosis: MβCD, a cholesterol-depleting cyclic oligomer of glycopiranoside was used as a general endocytosis inhibitor [23]; Cpz, a cationic amphipathic molecule, was used to inhibits formation of clathrin-coated pits [24]; Gen, a specific tyrosine kinase inhibitor that causes local disruption of the actin cytoskeleton and avoids recruiting of dynamin II, was used as caveolin-mediated endocytosis and Rho-mediated endocytosis inhibitor [25,26]; Wort that blocks PI3-kinase and inhibits the fusion of membrane protrusions, was used as macropinocytosis and phagocytosis inhibitor [27]; CytD, that disrupts actin filaments and inhibits actin polymerization and membrane ruffling, was used as phagocytosis and pinocytosis inhibitor [28]; CQ, a weak base that increases endosomal and lysosomal pH, cause lysosomal disruption [29] and reduction of clathrin-dependent endocytosis [30]; and Noc, that disrupts microtubules and inhibits translocation of endosomes and lysosomes [31], blocking clathrin-dependent endocytosis, not affecting SV40 uptake to caveosomes, but affects vesicular movements into the cell [32]. However, the inhibitors of endocytosis are also cytotoxic drugs, for example MβCD destroys the cell membrane, Noc is an anti-neoplastic agent and Wort inhibits DNA repair and cell proliferation. Hence, before starting with the inhibition assay, their cytotoxicity as function of concentration and incubation time must be screened on each cell type. Our preliminary findings showed that MβCD, Gen, CQ and Noc were more toxic on Sk-Mel-28 cells than on HaCaT cells, therefore the assay on Sk-Me-28 cells was carried out at lower inhibitors concentrations that the used in HaCaT cells.

According to the cytoxicity of inhibitors on both cell types (Fig. 5), the inhibition assay was performed at the maximal inhibitor concentration rendering viability higher than 75–80%. Sk-Mel-28 cells resulted extremely sensitive to the combination of G5G2.5 and MβCD or Gen, being these inhibitors excluded from the assay.

Our findings showed that in Sk-Mel-28 cells, the uptake of G5G2.5 and G6.5 significantly decreased when the endocytic processes were inhibited at 4 °C. CytD, Noc and Wort decreased 40, 20 and 45%, respectively, the uptake of G5G2.5. CQ and CytD decreased 30 and 20% respectively the uptake of G6.5 (Fig. 6B). Cpz did not affect the polymers uptake; however it decreased the uptake of the marker of clathrin-dependent endocytosis, Tf-Alexa-555. G5G2.5-FITC was seen as homogeneously distributed cytoplasmic dots (Fig. 7) of high (Pearson's correlation coefficient >0.5) (Fig. 8) co-localization with the macropinocytosis marker Dex-Alexa-568 and the lysosomal marker Lysotracker Red.

In HaCat cells, the uptake of G5G2.5 and G6.5 also significantly decreased when the endocytic processes were inhibited at 4 °C, but only CytD decreased 30% the uptake of G5G2.5. Wort, which decreased the uptake of the macropinocytosis marker dextran, and nocodazole, did not affect the uptake of none of the polymers (Fig. 6A). Cpz and CQ increased – instead of decreased – the uptake of both polymers. Other authors have reported that inhibition of clatrhin coated uptake may upregulate other pathways on the other hand, chlorpromazine, an amphipathic molecule, could affect the fluidity of the membrane in a positive way and therefore facilitating endocytosis. Additionally, Cpz did not reduce the uptake of Tf-Alexa-555; therefore the mediation of clathrin-dependent endocytosis could not be assessed. These results indicated that the

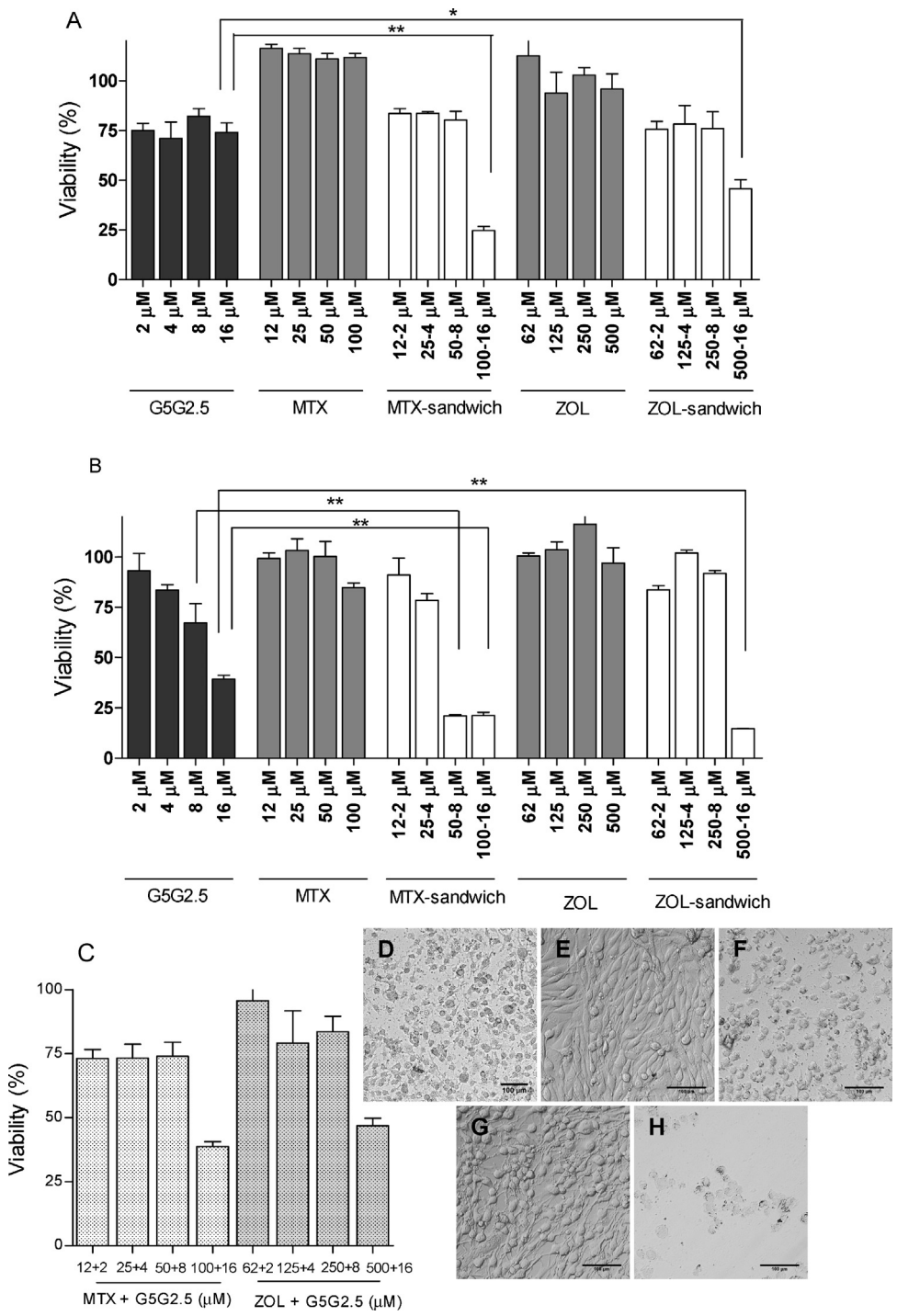

Fig. 3. Cytotoxicity of G5G2.5, free drugs, MTX- and ZOL-*sandwiches* on HaCaT (A) and Sk-Mel-28 cells (B). Cytotoxicity of simple mixtures of G5G2.5 and drugs on Sk-Mel-28 cells (C). Phase contrast microscopic images of Sk-Mel-28 cells incubated with 16 µM G5G2.5 (D); 100 µM MTX (E); 50–8 µM MTX-*sandwich* (F); 500 µM ZOL (G) and 500–16 µM ZOL-*sandwich* (H). Three independent experiments were completed for each measurement. Values are expressed as means ± S.D, $^{**}p < 0.01$, $^{*}p < 0.05$.

uptake of G5G2.5 depended on the dynamics of the actin cytoskeleton and excluded the mediation of macropinocytosis.

4. Discussion

In several pre-clinical approaches the covalent conjugation of MTX to different dendrimers was shown to be a suitable strategy to increase the plasma half-life and tumor accumulation of MTX [33,34]. Modifying pharmacokinetics and biodistribution however, may not be the unique ways of improving the antitumoral activity of MTX. For instance, Baker's group developed multifunctional PAMAM G5 dendrimers by conjugating MTX and folic acid (as a ligand of the folate receptor that it is over-expressed in different tumors, such as ovary, breast, colon and lung). When intravenously administered, these dendrimers reduce the tumoral growth, increase the animal survival and reduce the toxic effects of MTX in a murine model of tumor induced with epidermoid carcinoma KB cells [35,36]. Not all tumors, however, respond in the same way to the dendritic polymers. For instance, recent studies showed that murine B16-F10 melanoma cells are sensitive to MTX

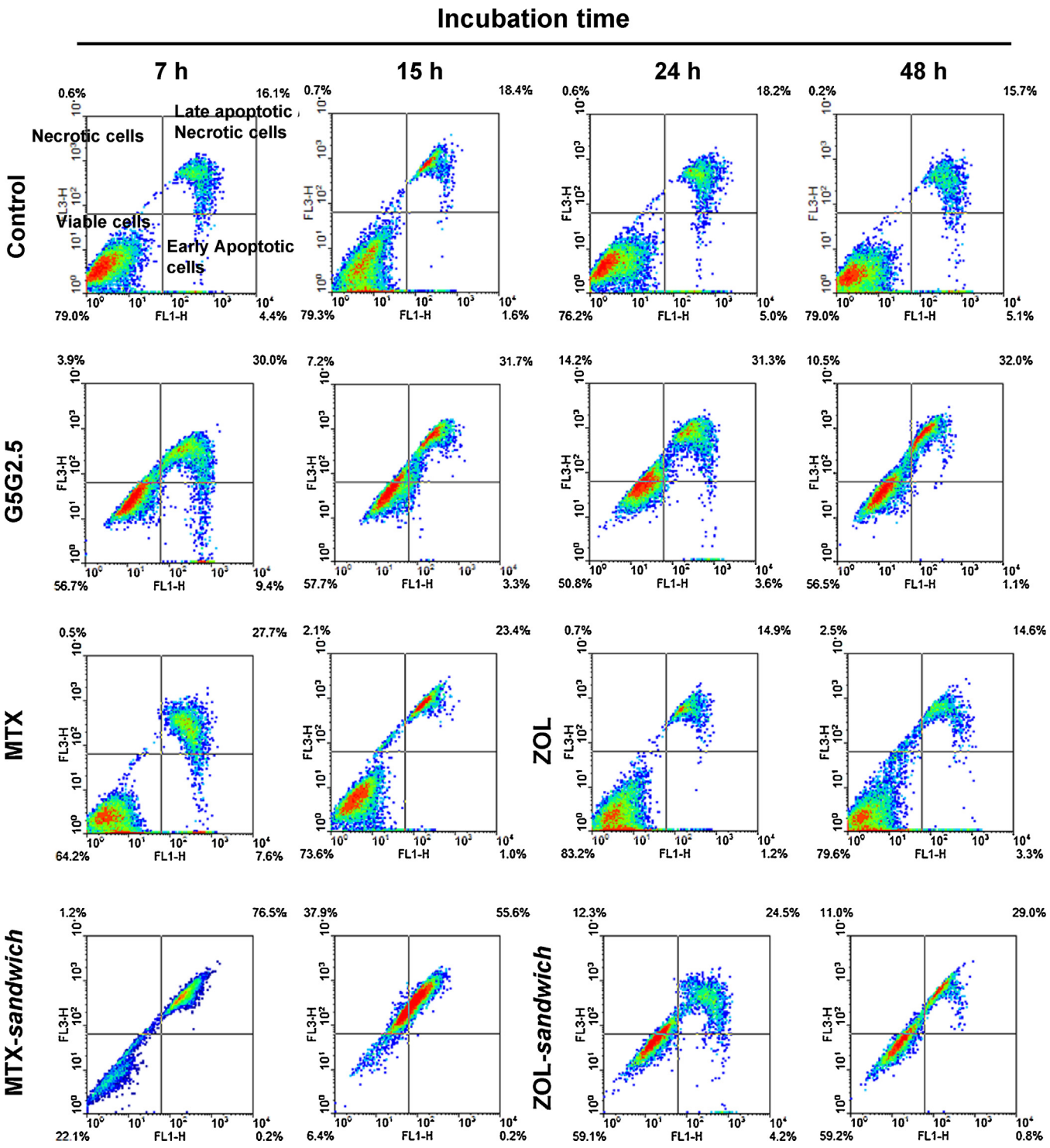

Fig. 4. Representative density plot diagrams of apoptosis/necrosis assay on SK-Mel-28 cells. Cells were incubated with buffer (Control cells) for 7, 15, 24 and 48 h; 8 μM G5G2.5 for 7, 15, 24 and 48 h; 50 μM MTX and 50–8 μM MTX-*sandwiches* for 7 and 15 h; 250 μM ZOL and 250–8 μM ZOL-*sandwiches* for 24 and 48 h.

(300 nM reduce 80% cell viability) but these cells are incapable of taking up dendrimers, resulting these dendrimer-MTX conjugates not cytotoxic [37]. The cytotoxicity to melanoma cells, on the other hand, strongly depends on the origin of the cell line. For instance, MTX is not cytotoxic to human melanoma cells SK-Mel-1 [38]. Similarly, 20 μM MTX inhibits proliferation (it is cytostatic) but does not induce morphological changes associated to cell death (it is not cytotoxic) on Sk-Mel-28 cells, which recovered after the treatment is discontinued [11]. Here, we found that up to 100 μM, MTX was neither cytostatic nor cytotoxic (it did not inhibit cell proliferation, did not produce morphological changes up to 50 μM and did not induce apoptosis/necrosis) to Sk-Mel-28 cells. However, the cytotoxicity of the 50–8 μM MTX-*sandwich* increased from 25 to 80–100% (by MTT and YOPRO/IP) the intrinsic cytotoxicity of 8 μM G5G2.5. The cytotoxicity was only induced on melanoma cells since the same *sandwich* did not affect the viability of HaCaT cells.

ZOL on the other hand, has been loaded in pegilated liposomes that after intravenous administration increased its tumoral

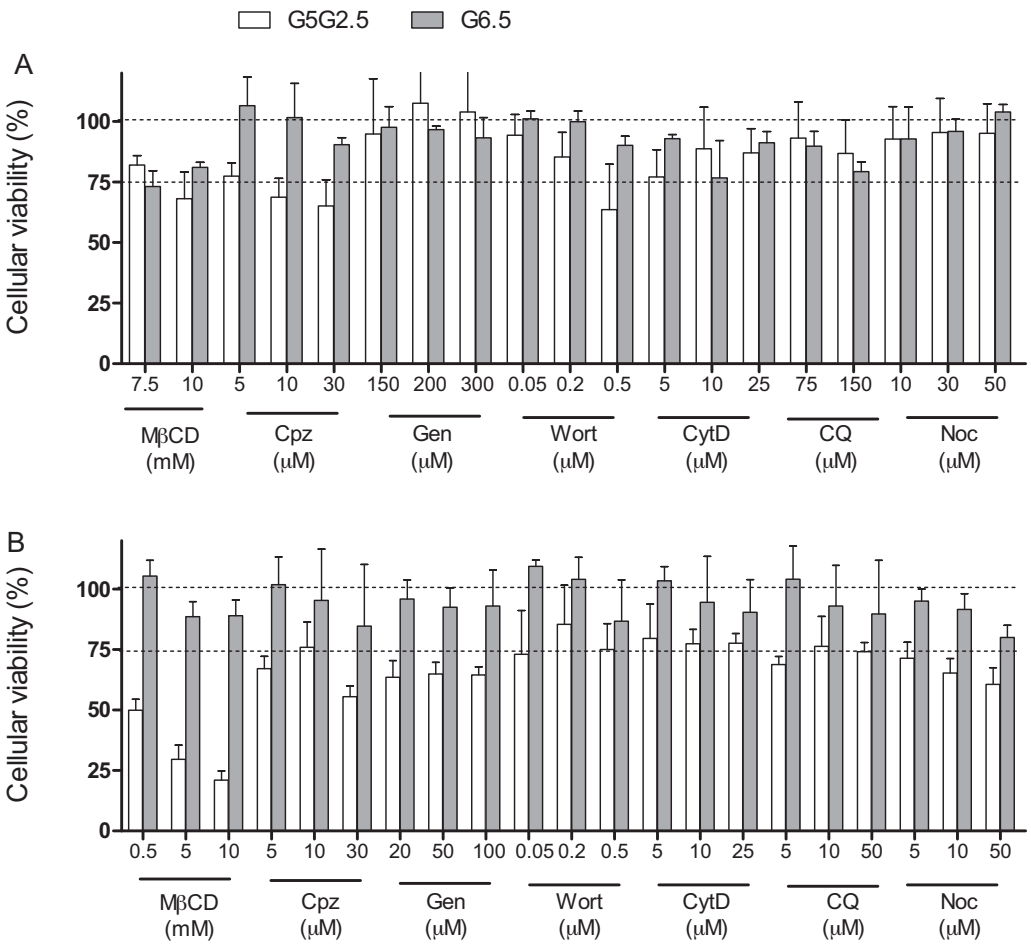

Fig. 5. Cytotoxicity of inhibitors of endocytosis and polymers on HaCaT (A) and SK-Mel (B) cells. Three independent experiments were completed for each measurement. Values are expressed as means ± S.D.

accumulation mostly due to the enhanced permeation and retention (EPR) effect [39,40]. To the best of our knowledge, this is the first time that ZOL is loaded within dendritic polymers. The cytotoxicity of ZOL is strongly dependent on the melanoma cell line.

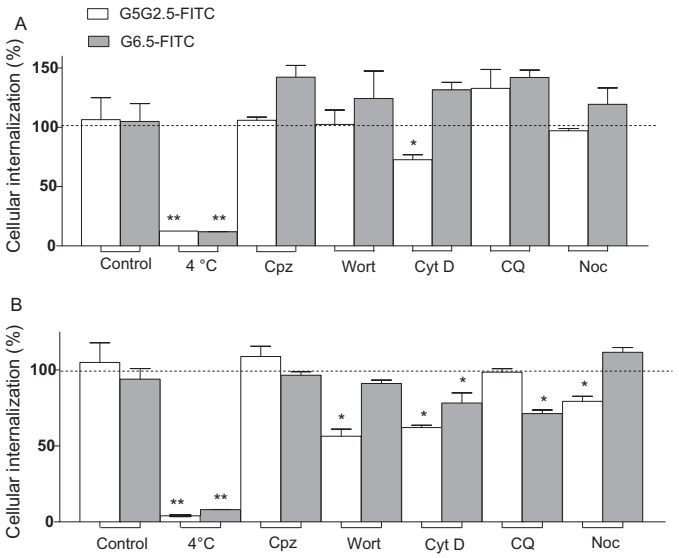

Fig. 6. Effect of inhibitors of endocytosis on uptake of G5G2.5-FITC and G6.5-FITC by HaCaT (A) and Sk-Mel-28 cells (B). Values are expressed as means ± S.D. $^{*}P = 0.05$, $^{**}P = 0.01$.

For instance, its IC50 is 100 μM after 24 h incubation with A375 and M186 human melanoma cells [41], whereas their IC50 are 48 and 20 μM after 72 h incubation with M14 and M14+ cells, respectively [40]. Here, we found that up to 500 μM ZOL was not cytotoxic to Sk-Mel-28 cells after 24 h incubation. However, the cytotoxicity of the 500–16 μM ZOL-*sandwich* was 85%, nearly 30% higher than the intrinsic cytotoxicity of 16 μM G5G2.5. And finally, altough the ZOL-*sandwich* was 35% more cytotoxic to Sk-Mel-28 cells than to HaCaT cells, the cytotoxicity to HaCaT cells was also high (50%).

These results suggested that above a minimal concentration, the *sandwiches* were more cytotoxic than free drugs, tecto-dendrimers alone and simple mixtures. Interestingly, the MTX-*sandwich* was more cytotoxic only to melanoma cells, while the ZOL-*sandwich* was more cytotoxic to melanoma cells and keratinocytes, as compared to the free drugs and tecto-dendrimers alone.

Previous studies have shown that the nature of the surface groups of dendrimers influences their uptake mechanism in different cell types [42]. Searching for a potential correlation between the selective cytotoxicity of tecto-dendrimers (and *sandwiches*) and their uptake mechanism, we screened the effect of a set of chemical inhibitors of endocytosis on the uptake of G5G2.5 by HaCaT and Sk-Mel-28 cells. In some cases, the relative technical simplicity of this approach is out weighted by uncertainties, such as: the opening of alternative uptake mechanism as a response to the inhibition; the non-specificity of the inhibitors (which depend on the cell type); and the intrinsic cytotoxicity of the inhibitors, leading to reducing the inhibitor concentration below their threshold levels of activity [43]. Our results showed that each cell type internalized tecto-dendrimers and G6.5 by different mechanisms. The

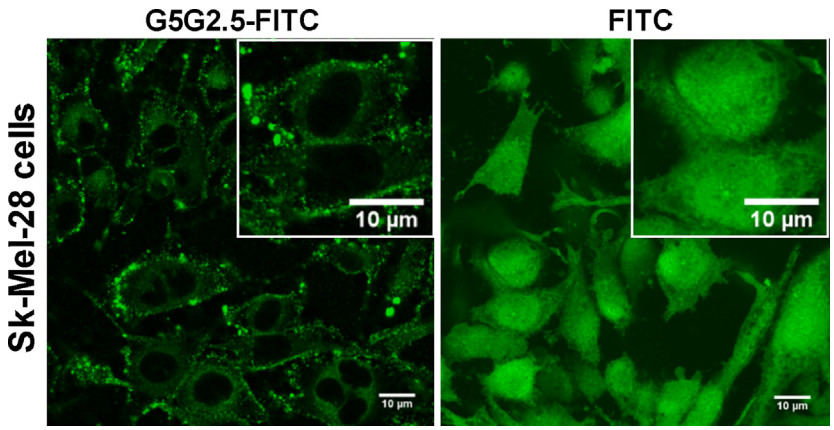

Fig. 7. Confocal laser scanning microscopic images of Sk-Mel-28 cells incubated with G5G2.5-FITC and FITC at 37 °C for 1 h.

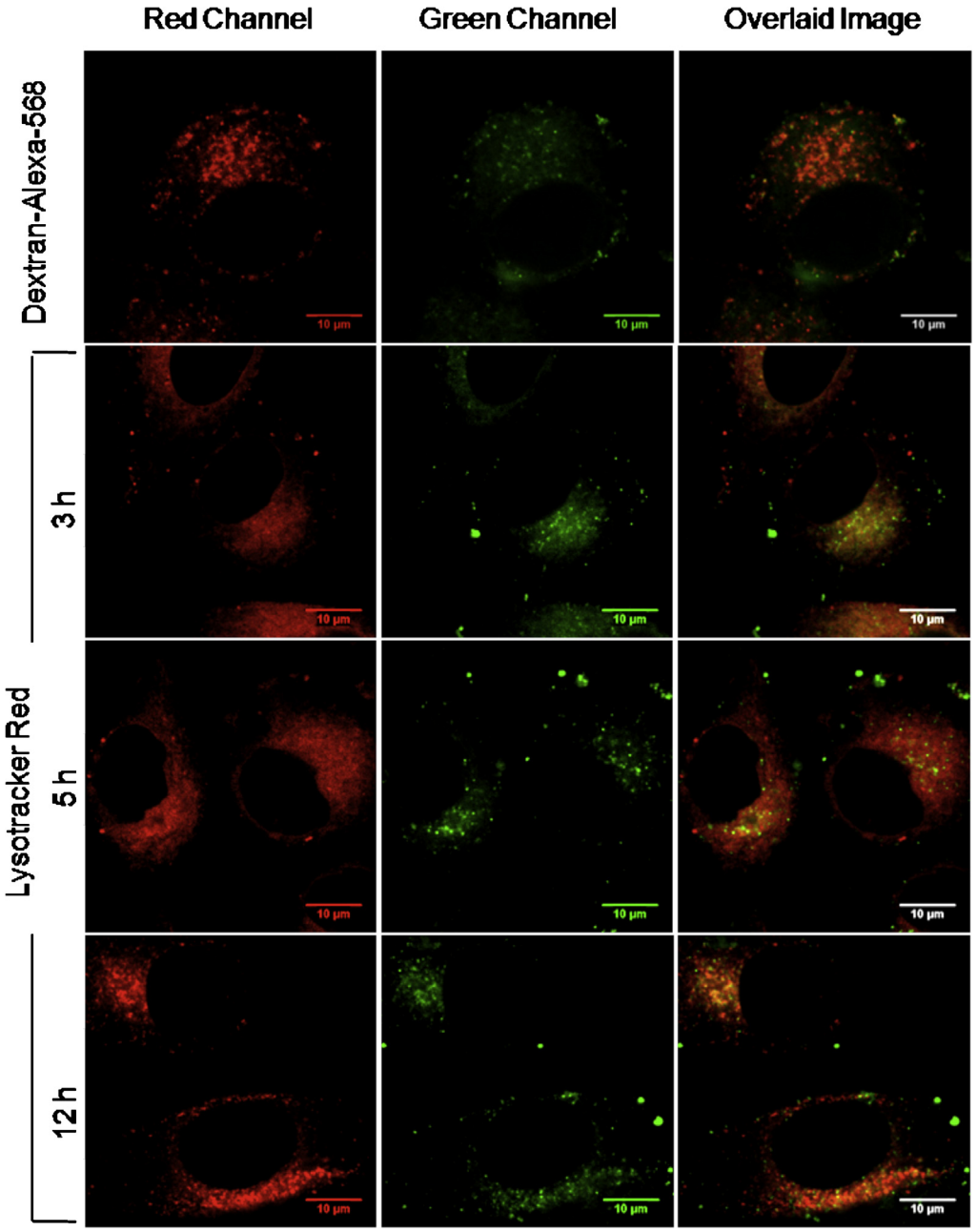

Fig. 8. Confocal laser scanning microscopic images of Sk-Mel-28 cells incubated with G5G2.5-FITC and co-incubated with Dextran-Alexa-568 or with Lysotracker Red for 3, 5 and 12 h.

uptake of G6.5 depended on the dynamics of the actin cytoskeleton and lysosomal acidification, in spite of no being mediated by clathrin-mediated endocytosis. The uptake of G5G2.5 on the other hand, depended on the dynamics of the actin cytoskeleton and on the microtubular assembly, which together with the inhibition by Wort and co-localization studies suggested a mechanism compatible with macropinocytosis in Sk-Mel-28 cells. Tecto-dendrimers possess a structure simmilar to G6.5 (simmilar molecular weight and hydrodynamic size 1,061,967 Da and 7–8 nm, respectively). However, theoretically 240 carboxylic groups would be at the surface of G5G2.5 if we assume that half of the surface groups of each PAMAM G2.5 are exposed. In comparison, the densely packed surface of G6.5 exposes 512 surface carboxylic groups. Hence difference in suface groups' density of G5G2.5 and G6.5 could be one reason of difference in uptake mechanisms.

Macropinocytosis, fluid-phase uptake modality employed by virtually any cell with exceptions of macrophages and brain microvessel endothelial cells [44,45], has been reported for dendrimers that utilize multiple mechanisms for cellular entry. For instance G3 is taken up by caveolin-mediated endocytosis and macropinocytosis in human intestinal adenocarcinoma cells (HT-29) [42]. Moreover, G2, G4 and G6 (neutral, cationic and lipidated) dendrimers are taken up by clathrin-mediated endocytosis and macropinocytosis in HeLa cells [46]. Although the macropinosomal traffic differs with the cell type and the triggering ligand, the macropinosomes maturate in a pathway parallel to classical endosomes that involves acidification and marker proteins. Macropinosomes would fuse between each other, late endosomes or lysosomes [47]. We have previously shown that G5G2.5 induces oxidative stress in Sk-Mel-28 cells, a potential cause of the selective cytotoxicity on these cells [20]. Now our results suggested that G5G2.5 and not close similar polymers such as G6.5, could access the macropinosomes. Probably part of the MTX entered the SK-Mel-28 cells by macropinocytosis of MTX-*sandwiches* and not by interaction with FRα. This switch of internalization pathway would allow deviating MTX from its exocytosis within melanosomes, enabling the cytoplasmic delivery of MTX and subsequent inhibition of DHFR. This would explain the higher cytotoxicity of the MTX sandwiches compared to the free drug. Different to MTX, ZOL is not taken up by a specific receptor; in osteoclast and J774 macrophages, ZOL is taken up by pynocytic mechanisms while in other cells ZOL diffuse very poorly. We propose that the higher toxicity of ZOL-*sandwich* as compared to free ZOL was due to an increased accumulation of ZOL, following its endocytic uptake as *sandwich* instead of free ZOL diffusion.

5. Conclusion

MTX and ZOL-*sandwiches* strongly increase the cytotoxicity of the free drugs in a cell type dependent modality. A further cost-benefit analysis would help to choose the more suitable sandwich for *in vivo* studies. The MTX-*sandwiches* were only toxic to melanoma, but the death of keratinocytes caused by ZOL-*sandwiches* could be an acceptable cost to pay in order to eliminate the malignant cells.

Acknowledgments

This work was supported by EULANEST project Nanoskin and Secretaria de Investigaciones, Universidad Nacional de Quilmes. PS has a fellowship from National Council for Scientific and Technological Research (CONICET) and GC has a fellowship from CIN. ELR and MJM are members of the Research Career Program from CONICET.

References

[1] V. Gray-Schopfer, C. Wellbrock, R. Marais, Melanoma biology and new targeted therapy, Nature 445 (2007) 851.
[2] T.B. Fitzpatrick, The biology of pigmentation, Birth Defects Orig. Artic. Ser. 7 (1971) 5.
[3] J.J. Nordlund, R.E. Boissy, The biology of melanocytes, in: R.K. Freinkel, D.T. Woodley (Eds.), The Biology of the Skin, Parthenon Publishing, New York, 2001 (Chapter 7).
[4] A. Haaka, G.A. Scott, Structure and function of the skin: overview of the epidermis and dermis, in: R.K. Freinkel, D.T. Woodley (Eds.), The Biology of the Skin, Parthenon Publishing, New York, 2001 (Chapter 2).
[5] T.R. Velho, Metastatic melanoma – a review of current and future drugs, Drugs Context (2012) 212242.
[6] B. Bandarchi, L. Ma, R. Navab, A. Seth, G. Rasty, From melanocyte to metastatic malignant melanoma, Dermatol. Res. Pract. (2010) 1.
[7] L. Sanchez del Campo, M.F. Montenegro, M. Saez-Ayala, M.P. Fernández-Pérez, J. Cabezas-Herrera, J.N. Rodriguez-Lopez, Cellular and molecular mechanisms of methotrexate resistance in melanoma, in: H.T. Duc (Ed.), Melanoma – From Early Detection to Treatment, InTech, 2013 (Chapter 14).
[8] W.A. Bleyer, J.A. Nelson, B.A. Kamen, Accumulation of methotrexate in systemic tissues after intrathecal administration, J. Pediatr. Hematol. Oncol. 19 (1997) 530.
[9] J. Grim, J. Chladek, J. Martinkova, Pharmacokinetics and pharmacodynamics of methotrexate in non-neoplastic diseases, Clin. Pharmacokinet. 42 (2003) 139.
[10] D.W. Kufe, M.M. Wick, H.T. Abelson, Natural resistance to methotrexate in human melanomas, J. Invest. Dermatol. 75 (1980) 357.
[11] L. Sánchez-del-Campo, M.F. Montenegro, J. Cabezas-Herrera, J.N. Rodríguez-López, The critical role of alpha-folate receptor in the resistance of melanoma to methotrexate, Pigment Cell Melanoma Res. 22 (2009) 588.
[12] K.G. Chen, M.M. Gottesman, in: V.J. Hearing, S.P.L. Leong (Eds.), From Melanocytes to Malignant Melanoma: the Progression to Malignancy, Humana Press, New Jersey, 2005 (Chapter 33).
[13] Z. Cheng, R.D. Singh, D.L. Marks, R.E. Pagano, Membrane microdomains, caveolae, and caveolar endocytosis of sphingolipids, Mol. Membr. Biol. 23 (2006) 101.
[14] J.R. Green, Bisphosphonates: preclinical review, Oncologist 9 (2004) S3.
[15] J.R. Green, A. Guenther, The backbone of progress – preclinical studies and innovations with zoledronic acid, Crit. Rev. Oncol. Hematol. 77 (2011) S3.
[16] I. Benzaïd, H. Mönkkönen, V. Stresing, E. Bonnelye, J. Green, J. Mönkkönen, J.L. Touraine, P. Clézardin, High phosphoantigen levels in bisphosphonate-treated human breast tumors promote V(9V(2 T-cell chemotaxis and cytotoxicity *in vivo*, Cancer Res. 71 (2011) 4562.
[17] A. Guenther, S. Gordon, M. Tiemann, R. Burger, F. Bakker, J.R. Green, W. Baum, A.J. Roelofs, M.J. Rogers, M. Gramatzki, The bisphosphonate zoledronic acid has antimyeloma activity in vivo by inhibition of protein prenylation, Int. J. Cancer 126 (2010) 239.
[18] P.D. Ottewell, D.V. Lefley, S.S. Cross, C.A. Evans, R.E. Coleman, I. Holen, Sustained inhibition of tumor growth and prolonged survival following sequential administration of doxorubicin and zoledronic acid in a breast cancer model, Int. J. Cancer 126 (2010) 522.
[19] A.C. Hirbe, A.J. Roelofs, D.H. Floyd, H. Deng, S.N. Becker, L.G. Lanigan, A.J. Apicelli, Z. Xu, J.L. Prior, M.C. Eagleton, D. Piwnica-Worms, M.J. Rogers, K. Weilbaecher, The bisphosphonate zoledronic acid decreases tumor growth in bone in mice with defective osteoclasts, Bone 44 (2009) 908.
[20] P. Schilrreff, C. Mundiña-Weilenmann, E.L. Romero, M.J. Morilla, Selective cytotoxicity of PAMAM G5 core-PAMAM G2.5 shell Tecto-dendrimers on melanoma cells, Int. J. Nanomed. 7 (2012) 4121.
[21] C.J.F. Bötcher, C.M. Van Gent, C. Pries, A rapid and sensitive sub-micro phosphorus determination, Anal. Chim. Acta. 24 (1961) 203.
[22] V. Zinchuk, O. Zinchuk, Quantitative colocalization analysis of confocal fluorescence microscopy images, Curr. Protoc. Cell Biol. (2008) 19.
[23] A. Subtil, I. Gaidarov, K. Kobylarz, M.A. Lampson, J.H. Keen, T.E. McGraw, Acute cholesterol depletion inhibits clathrin coated pit budding, Proc. Natl. Acad. Sci. USA 96 (1999) 6775.
[24] L.H. Wang, K.G. Rothberg, R.G. Anderson, Mis-assembly of clathrin lattices on endosomes reveals a regulatory switch for coated pits formation, J. Cell Biol. 123 (1993) 1107.
[25] R.G. Parton, B. Joggerst, K. Simons, Regulated internalization of caveolae, J. Cell Biol. 127 (1994) 1199.
[26] I.R. Nabi, P.U. Le, Caveolae/raft-dependent endocytosis, J. Cell Biol. 161 (2003) 673.
[27] N. Araki, M.T. Johnson, J.A. Swanson, A role for phosphoinositide 3-kinase in the completion of macropinocytosis and phagocytosis by macrophages, J. Cell Biol. 135 (1996) 1249.
[28] B. Qualmann, M.M. Kessels, R.B. Kelly, Molecular links between endocytosis and the actin cytoskeleton, J. Cell Biol. 150 (2000) F111.
[29] A. Michihara, K. Toda, T. Kubo, Y. Fujiwara, K. Akasaki, H. Tsuji, Disruptive effect of chloroquine on lysosomes in cultured rat hepatocytes, Biol. Pharm. Bull. 28 (2005) 947.
[30] D.D. Pless, R.B. Wellner, In vitro fusion of endocytic vesicles: effects of reagents that alter endosomal pH, J. Cell Biochem. 62 (1996) 27.
[31] A. Subtil, A. Dautry-Varsat, Microtubule depolymerization inhibits clathrin coated-pit internalization in non-adherent cell lines while interleukin 2 endocytosis is not affected, J. Cell Sci. 110 (1997) 2441.

[32] L. Pelkmans, J. Kartenbeck, A. Helenius, Caveolar endocytosis of simian virus 40 reveals a new two-step vesicular-transport pathway to the ER, Nat. Cell Biol. 3 (2001) 473.
[33] S.Y. Kong, G.T. Tang, Y.Y. Pei, Z. Jiang, Preparation and *in vitro* release of methotrexate complexation with PEGylated dendrimers, Chin. Pharm. J. 43 (2008) 1085.
[34] L.M. Kaminskas, B.D. Kelly, V.M. McLeod, B.J. Boyd, G.Y. Krippner, E.D. Williams, C.J. Porter, Pharmacokinetics and tumor disposition of PEGylated, methotrexate conjugated poly-L-lysine dendrimers, Mol. Pharm. 6 (2009) 1190.
[35] A. Quintana, E. Raczka, L. Piehler, I. Lee, A. Myc, I. Majoros, A.K. Patri, T. Thomas, J. Mulé, J.R. Baker Jr., Design and function of a dendrimer based therapeutic nanodevice targeted to tumor cells through the folate receptor, Pharm. Res. 19 (2002) 1310.
[36] I.J. Majoros, C.R. Williams, A. Becker, J.R. Baker Jr., Methotrexate delivery via folate targeted dendrimer-based nanotherapeutic platform, Wiley Interdiscip. Rev. Nanomed. Nanobiotechnol. 1 (2009) 502.
[37] H. Zong, T.P. Thomas, K.H. Lee, A.M. Desai, M.H. Li, A. Kotlyar, Y. Zhang, P.R. Leroueil, J.J. Gam, M.M. Banaszak Holl, J.R. Baker Jr., Bifunctional PAMAM dendrimer conjugates of folic acid and methotrexate with defined ratio, Biomacromolecules 13 (2012) 982.
[38] C.H. Shih, T.B. Chiang, W.J. Wang, Inhibition of integrins αv/α5-dependent functions in melanoma cells by an ECD-disintegrin acurhagin-C, Matrix Biol. 32 (2013) 152.
[39] H. Shmeeda, Y. Amitay, J. Gorin, D. Tzemach, L. Mak, J. Ogorka, S. Kumar, J.A. Zhang, A. Gabizon, Delivery of zoledronic acid encapsulated in folate-targeted liposome results in potent *in vitro* cytotoxic activity on tumor cells, J. Control Release. 146 (2010) 76.
[40] M. Marra, G. Salzano, C. Leonetti, M. Porru, R. Franco, S. Zappavigna, G. Liguori, G. Botti, P. Chieffi, M. Lamberti, G. Vitale, A. Abbruzzese, M.I. La Rotonda, G. De Rosa, M. Caraglia, New self-assembly nanoparticles and stealth liposomes for the delivery of zoledronic acid: a comparative study, Biotechnol. Adv. 30 (2012) 302.
[41] A.M. Forsea, C. Müller, C. Riebeling, C.E. Orfanos, C.C. Geilen, Nitrogen-containing bisphosphonates inhibit cell cycle progression in human melanoma cells, Br. J. Cancer. 91 (2004) 803.
[42] A. Saovapakhiran, A. D'Emanuele, D. Attwood, J. Penny, Surface modification of PAMAM dendrimers modulates the mechanism of cellular internalization, Bioconjug. Chem. 20 (2009) 693.
[43] D. Vercauteren, J. Joanna Rejman, T.F. Martens, J. Demeester, S.C. De Smedt, K. Braeckmans, On the cellular processing of non-viral nanomedicines for nucleic acid delivery: mechanisms and methods, J. Control. Release 161 (2012) 566.
[44] S.D. Conner, S.L. Schmid, Regulated portals of entry into the cell, Nature 422 (2003) 37.
[45] J.A. Swanson, C. Watts, Macropinocytosis, Trends Cell Biol. 5 (1995) 424.
[46] L. Albertazzi, M. Serresi, A. Albanese, F. Beltram, Dendrimer internalization and intracellular trafficking in living cells, Mol. Pharm. 7 (2010) 680.
[47] J. Mercer, A. Helenius, Gulping rather than sipping: macropinocytosis as a way of virus entry, Curr. Opin. Microbiol. 15 (2012) 490.